ISSN 0915-633X

NATIONAL INSTITUTE FOR FUSION SCIENCE

An Option of ICRF Ion Heating Scenario in Large Helical Device

V. Vdovin, T. Watari and A. Fukuyama

(Received - Oct. 28, 1996)

NIFS-502 July 1997

RESEARCH REPORT
NIFS Series

NAGOYA, JAPAN

AN OPTION OF ICRF ION HEATING SCENARIO IN LARGE HELICAL DEVICE

V. Vdovin*, T. Watari

National Institute for Fusion Science,

Japan

A. Fukuyama

Okayama University,

Japan

*) on leave from Kurchatov Institute, Moscow

Abstract.

Specific behavior of confining magnetic field in Large Helical Device suppresses tokamak-like ion heating scheme for ion cyclotron plasma heating with outside ICRF antenna. Respectively, the basic ICRF scenario with D(H) plasma will heat the electrons, as have been shown in stellarator CHS experiments. To overcome this difficulty, we propose to use in LHD high magnetic field side antenna operating in "heavy" minority heating scenarios H(D) or H(He-3), where brackets indicate minority ions. We show analytically that predominantly heated in this scenario will be the minority ions, subsequently transferring their energy to bulk proton ions. Another proposed scenario operates with "light" ion minority scheme like D(H), but with addition of third isotope ion component like C^{13}, Ne^{21}, Li^{7}, etc. . These third isotope ions eliminate degeneration of second harmonic frequency with fundamental frequency of minority ion(H) or second harmonics of deuterium ions. Isotopic ions will be heated due to a mode converted Ion Bernstein Waves close to second harmonic ion cyclotron layer ($\omega=2\omega_{ci}$).

Key words:

Helical Device, stellarator, minority ions, tokamak, antenna, ion cyclotron heating, two ion hybrid resonance, Fast Waves, Ion Bernstein Waves.

I. Basic ICRF electron heating scenario in LHD

In Fig. 1a, we show magnetic field modules B contour lines and flux surfaces in LHD device, calculated with stellarator equilibrium code VMEC for high beta LHD plasma case of $<\beta> = 2\%$. In a basic ICRF heating scenario, it is planned to make use of outside loop antenna, as depicted in Fig. 1b. It is impossible to keep one of $\omega=\omega_{ci}$ resonance zone in a geometrical plasma center because the other resonance zone locates very close to the antenna region. Consequently, it was proposed since successful CHS ICRF experiments [2] to decrease generator frequency and to keep $\omega=\omega_{ci}$ resonance more closer to the top and bottom of a plasma with easily installed outside antenna (see Fig. 1b). In usual two ion species D(H) scenario (ion minority species in brackets), fast waves radiated from outside antenna will first meet two-ion-hybrid resonance. As well known from tokamak and CHS stellarator experiments, such heating scenario will lead to electron heating predominantly .

II. "Heavy" minority scenario with high field side antenna

To overcome this specific difficulty for ion heating due to peculiarity of a magnetic field configuration in helical devices like LHD, we propose a new heating scenario. High field side ICRF antenna as depicted on Fig. 2a, will be used. "Heavy" minority scenario like H(D) or H(He^3) will be employed by adding D or He-3 minority ions in bulk hydrogen plasma. More exact definition of "heavy" minority scenario will be given below. In this case, as it was recognized in tokamaks in eighties, the fast waves will firstly meet an ion cyclotron resonance layer $\omega=\omega_{cHe3}$ (or $\omega=\omega_{cD}$), thereby providing predominantly ion heating. In Fig. 2b, squared perpendicular refractive index is shown over a "major radius like coordinate R" along a path of continuously decreasing magnetic field. The interesting difference from "classical usual" D(H) scenario is absence of a "cut off" layer between cyclotron resonance layer ($\omega=\omega_{ci}$) and the conversion layer to Ion Bernstein Waves (IBW). It means also that small fraction of FW power, the part which is not absorbed at ion cyclotron zone, will be absorbed by electrons. We will prove these statements analytically in section IV.

We also propose to use two antenna operating at slightly different two frequencies, by which core plasma heating is maintained compensating the positional change of flux surfaces with respect to cyclotron layer with subsidiary help of intrinsic focussing effect . These antennae, located at high magnetic field sides have additional advantage, being electrically more strong, as was proved by

tokamak experience.

III. 3 component ion heating scenario with high field side antenna

The above high field side antenna can provide another ion heating regime with "light" minority scenario D(H) and D(He3), if a third isotope ion component like C^{13}, Ne^{21}, Li^{7}, etc. are added. Degeneration of cyclotron frequencies between $\omega_{c,H}$, $2\omega_{c,D}$, $2\omega_{c,Li}$, $2\omega_{c,Ne}$, $2\omega_{c,C}$ are resolved due to the different charge to mass ratios. Dispersion curve for a plasma with these "heavy" and fortunately stable isotopes, is illustrated in Fig. 3. The launched wave experience very weak absorption as it passes through $\omega = 2\omega_{ci}'$ layer as FW, where prime means an isotope minority. However, absorption at $\omega = 2\omega_{c,i}'$ is enhanced as the wave passes through it again after mode converted to IBW waves; IBW is predominantly electrostatic wave and has large left hand component of electric field. These high Z isotopes (Z_{C13}= 6, Z_{Ne21}=10) ions are very collidable due to Z^2 dependence. It means that: 1) their ion distribution function will be sufficiently isotropic, an important factor for stellarator cases with regard to its loss cones, and 2) they transfer their energy mainly to bulk plasma ions, because their energy is likely to satisfy $W < W_{critical}$.

These isotope 3-ion component schemes have been partly investigated in T-10 tokamak[3] with outside antenna and in TFR experiments with inside antenna[4].

IV. Theoretical consideration of "heavy" minority scenario

4.1 *Dispersion*

In this section we will give an analytical consideration of two ion component ICRF heating scenarios with "heavy" minority ions. The transverse refractive index ($N_\perp = k_\perp c/\omega$) for Fast Wave is given by

$$N_\perp^2 = \frac{(\varepsilon_1 - n_\parallel^2)^2 - \varepsilon_2^2}{\varepsilon_1 - n_\parallel^2} \qquad (1)$$

, where for a cold plasma

$$\varepsilon_1 = 1 - \sum_{\alpha} \frac{\omega_{p\alpha}^2}{\omega^2 - \omega_{c\alpha}^2} \qquad (2)$$

and

$$\varepsilon_2 = -\sum_{\alpha} \frac{\omega_{p\alpha}^2}{\omega^2 - \omega_{c\alpha}^2} \frac{\omega_{c\alpha}}{\omega} \quad . \qquad (3)$$

Here, the summation with respect to α is taken over e and i. We rewrite these tensor components in more convenient forms as

$$\varepsilon_1 = -N_A^2(x)\left(\frac{\mu_1}{\Omega_1^2 - 1} + \frac{\mu_2}{\Omega_2^2 - 1}\right) \qquad (4)$$

and

$$\varepsilon_2 = -N_A^2(x)\left(\frac{\mu_1}{\Omega_1^2 - 1}\Omega_1 + \frac{\mu_2}{\Omega_2^2 - 1}\Omega_2\right) \qquad (5)$$

, where

$$\Omega_{1,2}(x) = \frac{\omega}{\omega_{c1,2}}, \quad \mu_1 = \frac{n_{i1}}{n_e}\frac{m_{i1}}{m_p}, \text{ and } \quad \mu_2 = \frac{n_{i2}}{n_e}\frac{m_{i2}}{m_p}. \qquad (6)$$

Here, Alfven refractive index is defined for a proton plasma as

$$N_A^2(x) = \frac{4\pi n_e(x) m_p}{B_0^2} \equiv \frac{c^2}{V_{Ap}^2} \qquad (7)$$

and estimated to be 30~50 in central parts of LHD plasma. The normalized frequencies, $\Omega_{1,2}$, depends on a space coordinate x due to the inhomogeneity of confining magnetic field $B_0(x)$; for a tokamak x would be taken in the direction of major radius.

4.2 *Analysis (heavy minority case)*

Let us take minority ion as first species and designate it by subscript 1. The majority ion is the second ion species designated by subscript 2. Since we are considering so called "heavy" minority case, $Z_1/m_1 < Z_2/m_2$ and $n_2 > n_1$. Cyclotron layer of minority ions, $\Omega_1 = 1$, is placed at the center of the plasma and $\Omega_2 < 1$ follows subsequently. Typical heavy minority regimes are H(D) and H(He-3).

It is convenient to expand two multipliers of the numerator in Eq.(1) to get the following form :

$$\varepsilon_1 \pm \varepsilon_2 - n_\parallel^2 = -N_A^2(x)\left(\frac{\mu_1}{\Omega_1^2 - 1}(1 \pm \Omega_1) + \frac{\mu_2}{\Omega_2^2 - 1}(1 \pm \Omega_2)\right) - n_\parallel^2, \qquad (8)$$

or

$$\varepsilon_1 \pm \varepsilon_2 - n_\parallel^2 = -N_A^2(x)\left(\pm\frac{\mu_1}{\Omega_1 \mp 1} \pm \frac{\mu_2}{\Omega_2 \mp 1} + \frac{n_\parallel^2}{N_A^2}\right). \qquad (9)$$

Then, Eq. (1) takes a form:

$$N_{\perp}^2 = N_A^2(x)\frac{\left(\dfrac{\mu_1}{\Omega_1 - 1} + \dfrac{\mu_2}{\Omega_2 - 1} + \dfrac{n_{\parallel}^2}{N_A^2}\right)\left(\dfrac{\mu_1}{1+\Omega_1} + \dfrac{\mu_2}{1+\Omega_2} - \dfrac{n_{\parallel}^2}{N_A^2}\right)}{\dfrac{\mu_1/2}{\Omega_1 - 1} + \dfrac{\mu_2}{\Omega_2^2 - 1} + \dfrac{n_{\parallel}^2}{N_A^2}} \quad . \quad (10)$$

Here, we claim again that "minority" is species 1: $\Omega_1 \approx 1$ and $\mu_1 << 1$. In the denominator, we put $\omega_1 + 1 \cong 2$ near of minority resonance and put the non resonant term $\Omega_2(z) \cong$ const. Now, one can easily see singularities and zeros in Eq. (10) and can draw spacial variation of the refractive index as shown in Fig. 4. Here, by analogy with tokamak, x coordinate may be called "major radius like coordinate".

Now we pay attention to the two domains where two important processes take place: near the cyclotron zone $\Omega_1 \approx 1$ and near the two ion hybrid resonance zone where $k_{\perp} \to \infty$. The latter corresponds to zero of denominator of Eq. (10).

One can see "singularity-cut off" pair as always refered to in light minority scensrios. However, there is an important difference from light minority case: the cut off is absent between cyclotron resonance zone and two ion hybrid resonance. The cut off $x = x_0^{\mathrm{Num}}$ is given by :

$$\frac{\mu_1}{\Omega_1 - 1} + \frac{\mu_2}{\Omega_2 - 1} + \frac{n_{\parallel}^2}{N_A^2} = 0$$

or

$$\Omega_1(x_0^{Num}) - 1 \cong \frac{x_0^{Num} - 1}{L} = \frac{\mu_1}{\dfrac{\mu_2}{1 - \Omega_2} - \dfrac{n_{\parallel}^2}{N_A^2(0)}} \quad . \quad (11)$$

Two ion hybrid resonance position, $x = x_0^{\mathrm{Den}}$, is given by :

$$\Omega_1(x_0^{Den}) - 1 \cong \frac{x_0^{Den} - 1}{L} = \frac{\mu_1/2}{\frac{\mu_2}{1-\Omega_2^2} - \frac{n_{\parallel}^2}{N_A^2(0)}} \quad . \tag{12}$$

Now we can calculate the separation between cut off and singularity :

$$\Delta x_{0\infty} = x_0^{\mathrm{Num}} - x_0^{\mathrm{Den}}$$

$$= \frac{\mu_1 L}{2D_{\mathrm{en}}} \left\{ \frac{\mu_2}{1+\Omega_2} + \frac{n_{\parallel}^2}{N_A^2(0)} \right\} \tag{13}$$

, where

$$D_{\mathrm{en}} \cong \frac{\mu_2^2}{(1-\Omega_2)(1-\Omega_2^2)} \quad . \tag{14}$$

Because usually $n_{//}^2 << N_A^2(0)$, Eq.(13) is given approximately by

$$\Delta x_{0\infty} \approx \frac{1}{2} \frac{\mu_1}{\mu_2} \mathrm{L}(1-\Omega_2)^2 \quad . \tag{15}$$

In all above formulas, L is characteristic length of magnetic field variation in plasma center region :

$$L = B_0 / \frac{dB_0}{dz} \Big|_{x=x_{res}} \quad . \tag{16}$$

Recalling that

$$\frac{\mu_1}{\mu_2} = \frac{n_1 m_1}{n_2 m_2} \quad \text{and} \quad n_e = Z_1 n_1 + Z_2 n_2 \tag{17}$$

, we have for two scenarios :

1) H(D) plasma : $\mu_1/\mu_2 = 2n_1/n_2$, $n_e = n_1 + n_2$, $\Omega_2 = 1/2$, and separation is :

$$\Delta x_{0\infty} = \frac{\nu}{2(1-\nu)} L \qquad (\nu = n_1/n_e) \qquad (18)$$

2) H(He-3) plasma : $\mu_1/\mu_2 = 3n_1/n_2$, $n_e = 2n_1 + n_2$, $\Omega_2 = 2/3$,

$$\Delta x_{0\infty} = \frac{\nu}{3(1-2\nu)} L . \qquad (19)$$

Thus, for H(He-3) scenario the cut off-singularity pair is closer in comparison with H(D) case by 1.5 times. It means that conversion of RF power to IBW, which is responsible for electron heating in ICRF experiments, will be much smaller in H(He-3) regime. As schematically shown in Fig. 6, in H(He-3) scenario fast waves are easily tunnel through the evanescent layer.

4.3 *Optical thickness for* $\omega = \omega_{ci}$'

Now we evaluate attenuation of fast waves passing through the Doppler broadened minority ions cyclotron zone. To do this, it is needed to add anti Hermitian parts to tensor components $\varepsilon_{1,2} \to \varepsilon_{1,2}^{(0)} + I\delta\varepsilon$ and to evaluate

$$\tau = 2\int \mathrm{Im} k_\perp dx \approx \frac{1}{3}\frac{n_1}{n_e} L \frac{\omega}{V_A} \quad . \qquad (20)$$

This evaluation is valid if concentration of minority ions is sufficiently small and polarization of the plasma is not influenced. More exactly, this criterion is given by

$$\frac{n_1}{n_e} < \frac{k_\parallel V_{Ti}^{(1)}}{\omega} \quad . \qquad (21)$$

If the minority concentration n_1 is greater then above critical value, two ion hybrid resonance effects must be taken into account.

For LHD parameters, Eq. (20) may be written in a form

$$\tau \approx \frac{10 n_1}{n_e}\left(\frac{L(cm)}{100cm}\right) \approx 0.5-1 \quad . \qquad (22)$$

It means that significant part of incident RF power will be absorbed during the first transit through the minority ion cyclotron layer. Non absorbed part will be partly converted to IBW, and partly tunnel through evanescent zone and propagate as a fast wave. After reflection from plasma boundary FW again tunnels back to the direction of minority cyclotron resonance layer. Important to stress is that the evanescent layer is 1.5 times shorter in H(He-3) scenario than in H(D) scenario. It means that FW easily tunnels, smaller RF power will be again converted and remaining FW power will be absorbed by minority ions.

4.4 *Role of Alfven resonance in "Heavy" minority scenario*

In previous analysis, we have been interested in phenomena near of plasma center, where ion cyclotron and hybrid resonances were placed in two ion component plasma. In "heavy" minority scenario, generator frequency is lower than cyclotron frequency of bulk ions. One may take that species 1 is hydrogenic ion and $\Omega_2<1$. In a such case the denominator in Eq. (4.1) has a second zero near of plasma boundary, where plasma density is much more rapidly changing in comparison with confining magnetic field. We clarify this situation introducing "minor radius" coordinate $x = R - R_0$ (in 3D plasma model it is magnetic flux psi-coordinate) to describe plasma density variations in Alfven refraction index. Now denominator of Eq. (1) have more detailed view :

$$N_{A0}^2(1-x^2)^{\alpha}\left\{\frac{\mu_1}{\Omega_1-1}+\frac{\mu_2}{\Omega_2^2-1}\right\}+n_{\parallel}^2=0 \qquad (23)$$

, wheret he first term in the parenthesis near of plasma boundary is negligible because here is no minority cyclotron resonance. It is easily studied that there is a second zero at the periphery of the plasma ($x\rightarrow 1$), which is well known Alfven resonance. The full dispersion curve over minor plasma cross section is shown on Fig. 6. Fast wave, radiated from inside antenna, meets Alfven resonance $\varepsilon_1(x) - n_{\parallel}^2 = 0$, followed by second zero of RHS numerator of of Eq.(10). We easily evaluate separation of this new "singularity -cut off" pair.

$$\Delta x_{0,\infty}^{(Alfven)} = \frac{a_0}{2}\left\{\frac{n_\parallel^2}{N_{A0}^2}\frac{1+\Omega_2}{\mu_2}\right\}^{1/\alpha}\left[1-(1-\Omega_2^2)^{1/\alpha}\right] \quad . \qquad (24)$$

The fast Wave, tunnelling through Alfven evanescent region, attenuates for typically small $n_\parallel^2/N_{A0}^2$ by the factor

$$E_y \approx E_0 exp\left\{-k_\parallel \Delta x_{0,\infty}^{(Alfv)}\right\} \quad . \qquad (25)$$

In stellarators $\alpha \approx 0.5 - 0.3$ (broad plasma density profiles) and

$$k_\parallel \Delta x_{0,\infty} \approx \frac{1}{2} k_\parallel a_0 \left(\frac{n_\parallel}{N_{A0}}\right)^{4-6} \ll 1 \quad . \qquad (26)$$

It means that Fast Wave going into Alfven resonance easily penetrates through the evanescent region. Convertion of RF power to Kinetic Alfven Waves is therefore negligibly small. ICRF antenna, however, must excite sufficiently small $k_{//}$ spectrum to ensure inequality $n_{//} \ll N_{A0}$ to be hold. It may be provided at least by a 2 loop antenna.

There is also another physical effect which can completely eliminate conversion of FW at Alfven resonance. At a plasma boundary there are impurity ions of first wall material together with partially stripped oxygen, nitrogen, carbon and etc.. Their cyclotron resonances are overlapped with Alfven resonance layer. Formally, it is evident from initial dispersion relation Eq. (1) that imaginary addition off them with reasonable (not very small) $k_{//}$ values eliminate Alfven resonance completely.

V. Conclusions

In this work we proposed two basic scenarios to heat directly ions in Large Helical Device. Main recommendation is to operate in multi-ion species regimes, providing variety of interesting ion heating schemes. The main proposed scheme involves operation with heavy minority ions in predominantly hydrogen plasma with deuterium or helium-3 ions, matching a generator frequency with minority ions cyclotron resonances. Crucial element of this scheme is ICRF antenna located at

high magnetic field side of the device. Dispersion of first Magnetosonic Waves in this scenario is such one that the first resonance to be met by waves is minority ion cyclotron resonance and thus predominant ion heating is provided. It was proposed to locate two ICRF high field side antennae in a toroidal section where plasma cross section is horizontally elongated in order to provide central RF power deposition profile against large Shafranov shift foreseen in high beta rexperiment.

The second scenario with high field side antenna uses classical D(H) or D(He-3) plasma with important addition of third ion isotopes component to eliminate degeneration with second harmonic of deuterium. The RF power, in this scenario, is absorbed as Ion Bernstein Wave at second harmonic resonance of third minority ions. High charge and masses of this third ion component will provide good transfer of absorbed power to the bulk plasma ions. Both schemes have been proved in tokamaks ICR experiments.

For successful operation in these scenarios antenna must provide needed $k_{\parallel}$ shaping with fortunately greater loading resistance.

Acknowledgments. Authors are greatly appreciated to discussion of related questions with Drs. R. Kumazwa, T. Seki and T. Mutoh. The help of Prof. O. Monticello (PPPL) in successful VMEC operation was very important.

References

[1] A. Iiyoshi, M. Fujiwara, O. Motojima, N. Ohyabu, K. Yamazaki, Fusion Technology, 17 (1990) 169

[2] S.Masuda, R.Kumazawa, K. Nishimura, T.Mutoh, T.Watari, et al., Nuclear Fusion, 37(1996)53

[3] V.V.Alikaev, E.L.Berezovskij, V.L.Vdovin, et al., proc. 12th European Conference on Controlled Fusion and Plasma Physics, Budapest, 1985, part-II, p-156

[4] TFR group, Nuclear Fusion, 26(1986)873

Figure captions

Fig.1 (a) the flux surfaces at troidal angle 0°; troidal angle is measured from a toroidal section where plasma cross section is vertically elongated. (b) mod-B contour with indication of

cyclotron- and two-ion-hybrid resonance layers. (c) flux surface and poloidal angle like coordinate for Shafranov shifted axis due to high-beta effect.

Fig.2 (a) Proposal of new antenna with heavy minority scenario. (b) Dispersion curve for the heavy minority regime.

Fig.3 Three component ion heating regime with High field side antenna. Addition of third impurity components provides variety of useful features.

Fig.4 Illustration of dispersion curve: (a) denominator of Eq(1) , (b) numerator of eq.(1), and (c) squared wave refractive index.

Fig.5 Illustration of the wave tunneling through the resonance cut/off pair. It is larger for He-3 majority case than for H majority scenario.

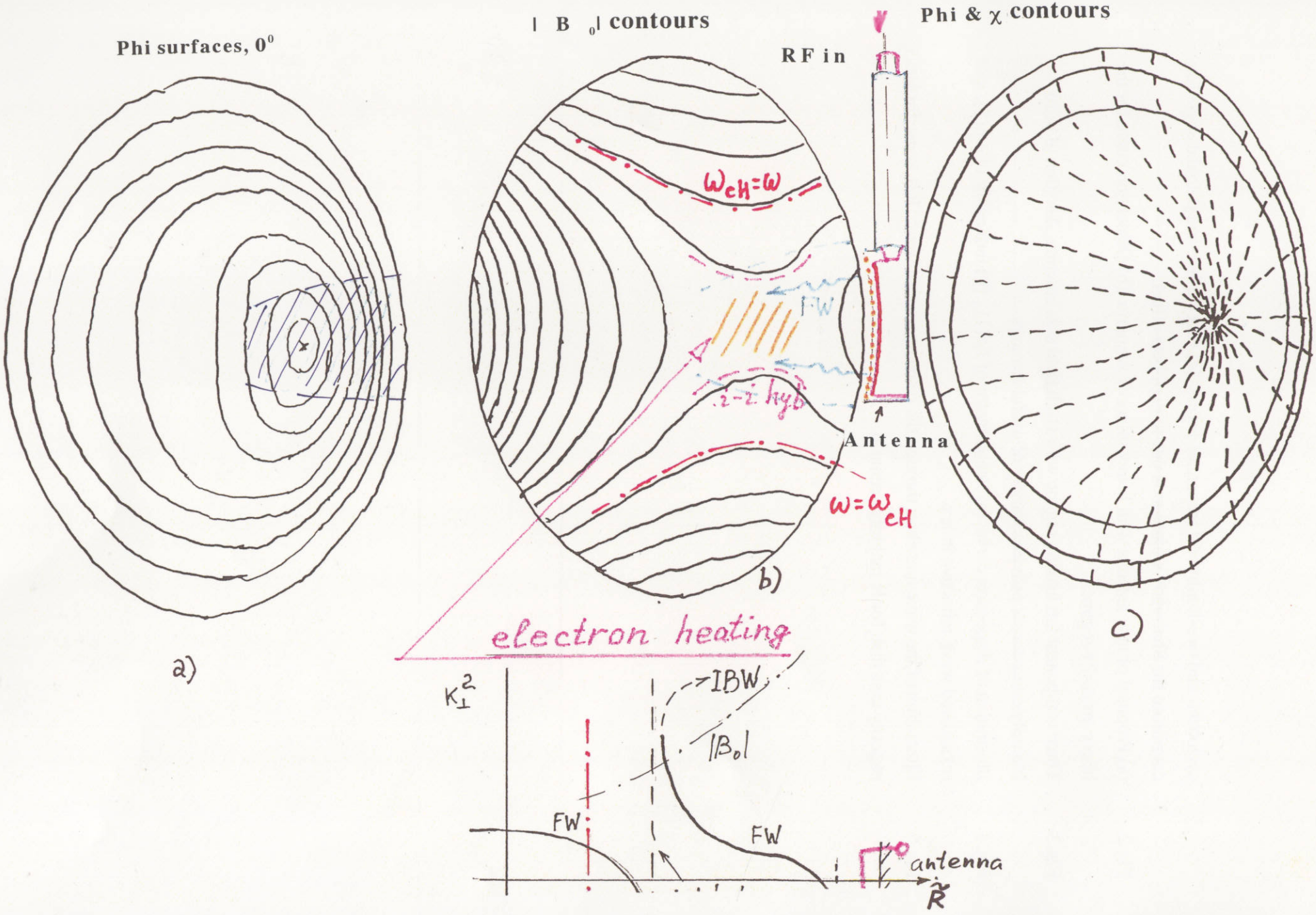
Phi surfaces, 0°
| B 0| contours
Phi & χ contours
RF in
ωcH=ω
FW
i-i hyb
Antenna
ω=ωcH
a)
b)
c)
electron heating
K⊥²
IBW
|B0|
FW
FW
antenna
R

Fig. 1

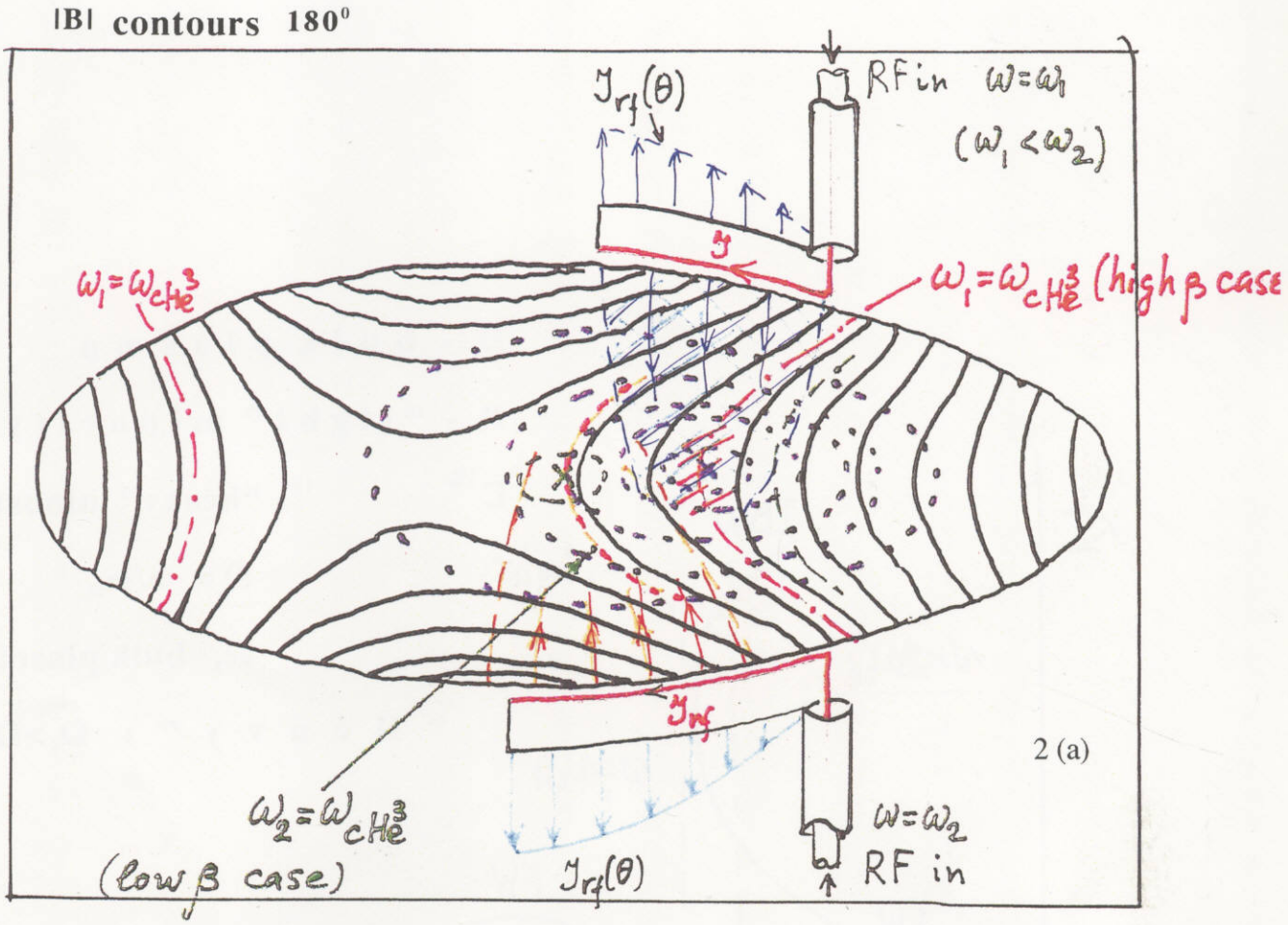

ION HEATING REGIME

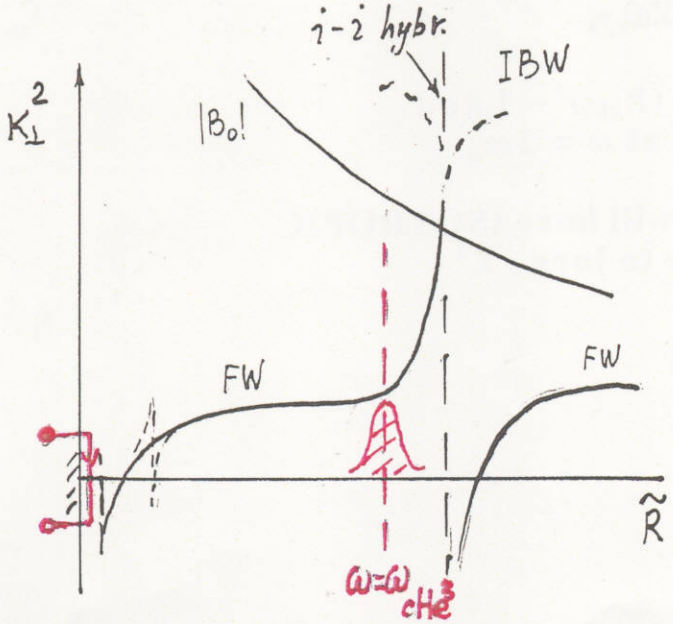

2 (b)

High density case

$n_{e0}=(5\text{-}10) \times 10^{19}\ m^{-3}$

$< k_{11} >_{ant} = 0.05\ cm^{-1}$

$H(5\%He^3)$ - plasma

$\omega = \omega_{cHe3}$

$(k_{11}\Delta r << 1)$

Fig. 2

D - bulk plasma

H - "light" minority

C^{13} ^{13} - "heavy" minority

$\Omega = \omega/\omega_{ci}$

Ω_2 - bulk plasma

"Heavy": $\Omega_1 > \Omega_2$

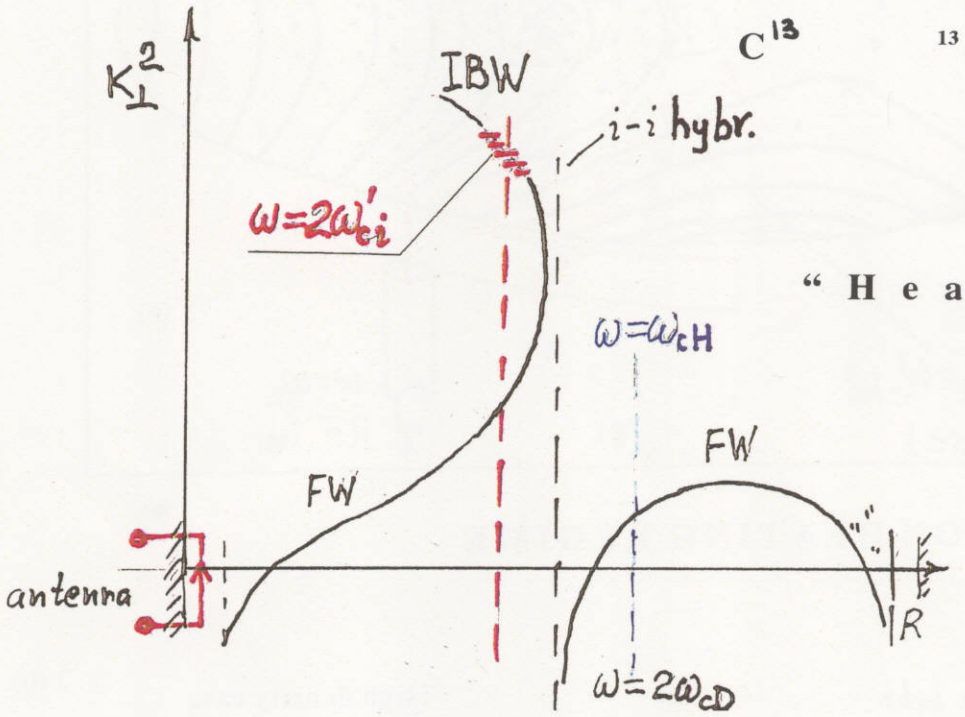

- Linearly polarized IBW has $(k_\perp \rho_i)^2 \sim 1$ and will be completely absorbed at $\omega = 2\omega_{ci}'$

- Heated minority isotop ions will have ISOTROPIC ion distribution function due to large Z^2

Fig. 3

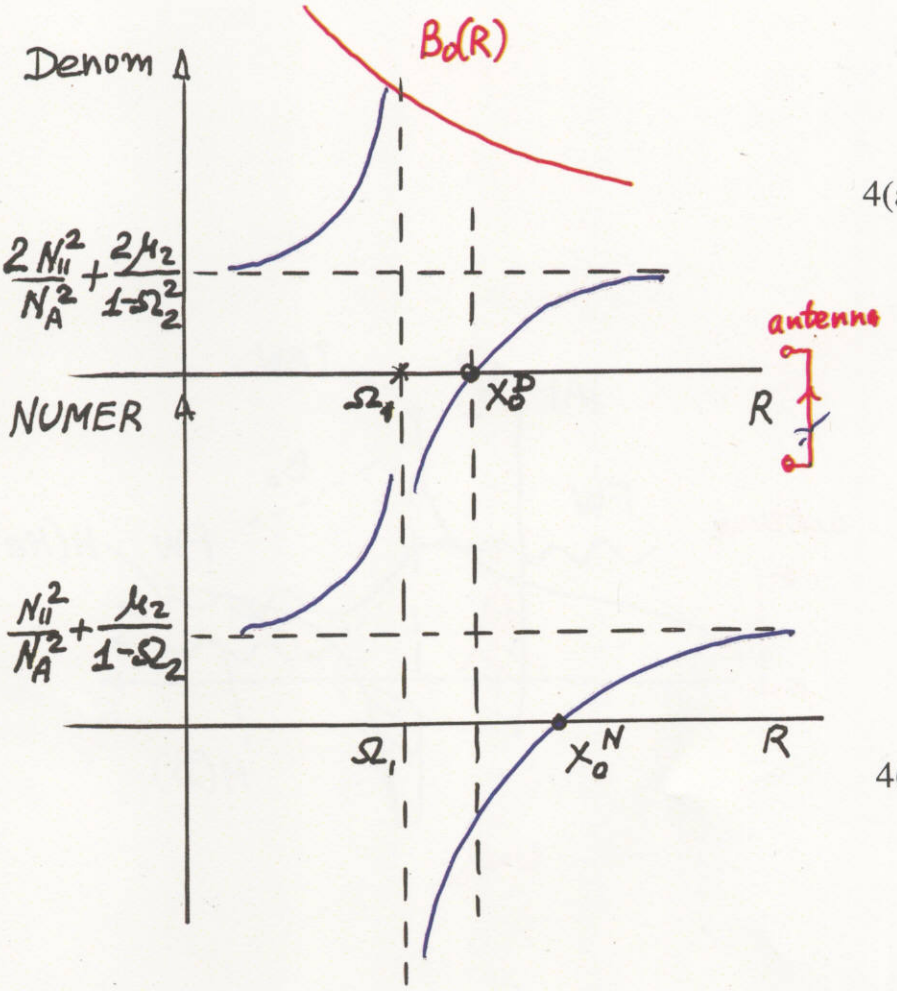
Denom
$B_0(R)$
$\frac{2N_{||}^2}{N_A^2}+\frac{2\mu_2}{1-\Omega_2^2}$
antenna
NUMER
Ω_1
X_0^D
R
$\frac{N_{||}^2}{N_A^2}+\frac{\mu_2}{1-\Omega_2}$
Ω_1
X_0^N
R

4(a)

4(b)

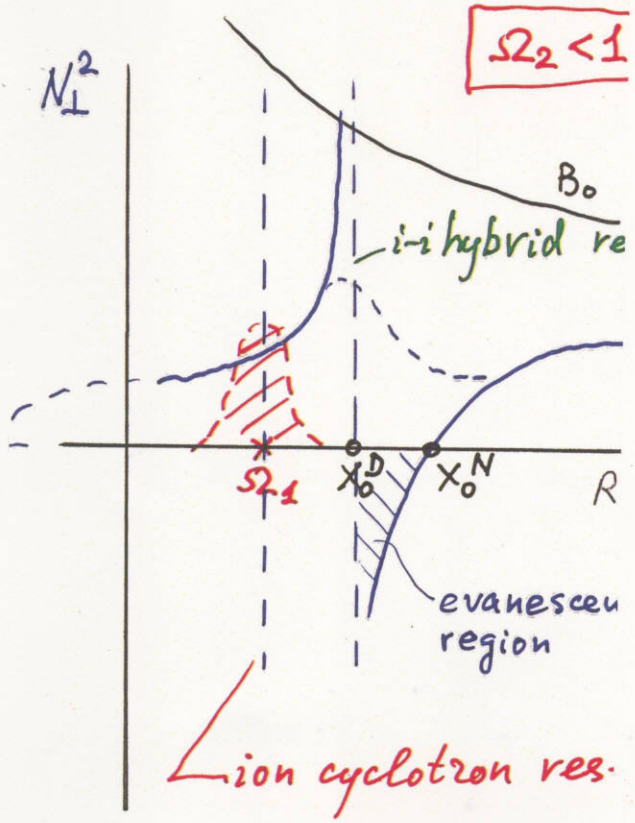
$\Omega_2<1$
$N_\perp^2$
B_0
i-i hybrid re
Ω_1
X_0^D
X_0^N
R
evanescen
region
ion cyclotron res.

4(c)

Fig. 4

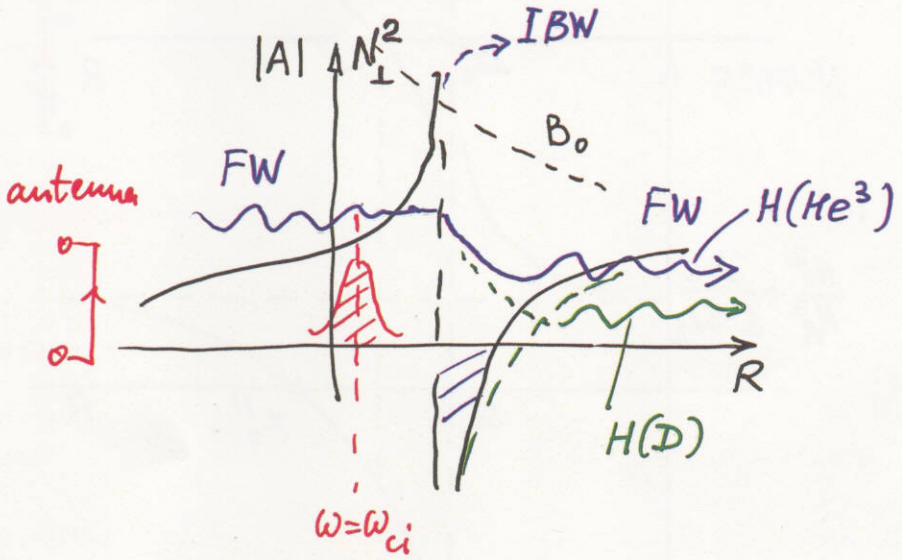

Fig. 5

Recent Issues of NIFS Series

NIFS-456 G Kawahara, S. Kida, M. Tanaka and S. Yanase,
Wrap, Tilt and Stretch of Vorticity Lines around a Strong Straight Vortex Tube in a Simple Shear Flow, Oct. 1996

NIFS-457 K. Itoh, S.- I. Itoh, A. Fukuyama and M. Yagi,
Turbulent Transport and Structural Transition in Confined Plasmas; Oct. 1996

NIFS-458 A. Kageyama and T. Sato,
Generation Mechanism of a Dipole Field by a Magnetohydrodynamic Dynamo; Oct. 1996

NIFS-459 K. Araki, J. Mizushima and S. Yanase,
The Non-axisymmetric Instability of the Wide-Gap Spherical Couette Flow; Oct. 1996

NIFS-460 Y. Hamada, A. Fujisawa, H. Iguchi, A. Nishizawa and Y. Kawasumi,
A Tandem Parallel Plate Analyzer; Nov. 1996

NIFS-461 Y. Hamada, A. Nishizawa, Y. Kawasumi, A. Fujisawa, K. Narihara, K. Ida, A. Ejiri, S. Ohdachi, K. Kawahata, K. Toi, K. Sato, T. Seki, H. Iguchi, K. Adachi, S. Hidekuma, S.Hirokura, K. Iwasaki, T. Ido, M. Kojima, J. Koong, R. Kumazawa, H. Kuramoto, T. Minami, I. Nomura, H. Sakakita, M. Sasao, K.N. Sato, T. Tsuzuki, J. Xu, I. Yamada and T. Watari,
Density Fluctuation in JIPP T-IIU Tokamak Plasmas Measured by a Heavy Ion Beam Probe; Nov. 1996

NIFS-462 N. Katsuragawa, H. Hojo and A. Mase,
Simulation Study on Cross Polarization Scattering of Ultrashort-Pulse Electromagnetic Waves; Nov. 1996

NIFS-463 V. Voitsenya, V. Konovalov, O. Motojima, K. Narihara, M. Becker and B. Schunke,
Evaluations of Different Metals for Manufacturing Mirrors of Thomson Scattering System for the LHD Divertor Plasma; Nov. 1996

NIFS-464 M. Pereyaslavets, M. Sato, T. Shimozuma, Y. Takita, H. Idei, S. Kubo, K. Ohkubo and K. Hayashi,
Development and Simulation of RF Components for High Power Millimeter Wave Gyrotrons; Nov. 1996

NIFS-465 V.S. Voitsenya, S. Masuzaki, O. Motojima, N. Noda and N. Ohyabu,
On the Use of CX Atom Analyzer for Study Characteristics of Ion Component in a LHD Divertor Plasma; Dec. 1996

NIFS-466 H. Miura and S. Kida,
Identification of Tubular Vortices in Complex Flows; Dec. 1996

NIFS-467 Y. Takeiri, Y. Oka, M. Osakabe, K. Tsumori, O. Kaneko, T. Takanashi, E. Asano, T. Kawamoto, R. Akiyama and T. Kuroda,
Suppression of Accelerated Electrons in a High-current Large Negative Ion Source; Dec. 1996

NIFS-468 A. Sagara, Y. Hasegawa, K. Tsuzuki, N. Inoue, H. Suzuki, T. Morisaki, N. Noda, O. Motojima, S. Okamura, K. Matsuoka, R. Akiyama, K. Ida, H. Idei, K. Iwasaki, S. Kubo, T. Minami, S. Morita, K. Narihara, T. Ozaki, K. Sato, C. Takahashi, K. Tanaka, K. Toi and I. Yamada,
Real Time Boronization Experiments in CHS and Scaling for LHD; Dec. 1996

NIFS-469 V.L. Vdovin, T.Watari and A. Fukuyama,
3D Maxwell-Vlasov Boundary Value Problem Solution in Stellarator Geometry in Ion Cyclotron Frequency Range (final report); Dec. 1996

NIFS-470 N. Nakajima, M. Yokoyama, M. Okamoto and J. Nührenberg,
Optimization of M=2 Stellarator; Dec. 1996

NIFS-471 A. Fujisawa, H. Iguchi, S. Lee and Y. Hamada,
Effects of Horizontal Injection Angle Displacements on Energy Measurements with Parallel Plate Energy Analyzer; Dec. 1996

NIFS-472 R. Kanno, N. Nakajima, H. Sugama, M. Okamoto and Y. Ogawa,
Effects of Finite-β and Radial Electric Fields on Neoclassical Transport in the Large Helical Device; Jan. 1997

NIFS-473 S. Murakami, N. Nakajima, U. Gasparino and M. Okamoto,
Simulation Study of Radial Electric Field in CHS and LHD; Jan. 1997

NIFS-474 K. Ohkubo, S. Kubo, H. Idei, M. Sato, T. Shimozuma and Y. Takita,
Coupling of Tilting Gaussian Beam with Hybrid Mode in the Corrugated Waveguide; Jan. 1997

NIFS-475 A. Fujisawa, H. Iguchi, S. Lee and Y. Hamada,
Consideration of Fluctuation in Secondary Beam Intensity of Heavy Ion Beam Prove Measurements; Jan. 1997

NIFS-476 Y. Takeiri, M. Osakabe, Y. Oka, K. Tsumori, O. Kaneko, T. Takanashi, E. Asano, T. Kawamoto, R. Akiyama and T. Kuroda,
Long-pulse Operation of a Cesium-Seeded High-Current Large Negative Ion Source; Jan. 1997

NIFS-477 H. Kuramoto, K. Toi, N. Haraki, K. Sato, J. Xu, A. Ejiri, K. Narihara, T. Seki, S. Ohdachi, K. Adati, R. Akiyama, Y. Hamada, S. Hirokura, K. Kawahata and M. Kojima,
Study of Toroidal Current Penetration during Current Ramp in JIPP T-IIU with Fast Response Zeeman Polarimeter; Jan., 1997

NIFS-478 H. Sugama and W. Horton,
Neoclassical Electron and Ion Transport in Toroidally Rotating Plasmas;

Jan. 1997

NIFS-479 V.L. Vdovin and I.V. Kamenskij,
3D Electromagnetic Theory of ICRF Multi Port Multi Loop Antenna; Jan. 1997

NIFS-480 W.X. Wang, M. Okamoto, N. Nakajima, S Murakami and N. Ohyabu,
Cooling Effect of Secondary Electrons in the High Temperature Divertor Operation; Feb. 1997

NIFS-481 K. Itoh, S.-I. Itoh, H. Soltwisch and H.R. Koslowski,
Generation of Toroidal Current Sheet at Sawtooth Crash; Feb. 1997

NIFS-482 K. Ichiguchi,
Collisionality Dependence of Mercier Stability in LHD Equilibria with Bootstrap Currents; Feb. 1997

NIFS-483 S. Fujiwara and T. Sato,
Molecular Dynamics Simulations of Structural Formation of a Single Polymer Chain: Bond-orientational Order and Conformational Defects; Feb. 1997

NIFS-484 T. Ohkawa,
Reduction of Turbulence by Sheared Toroidal Flow on a Flux Surface; Feb. 1997

NIFS-485 K. Narihara, K. Toi, Y. Hamada, K. Yamauchi, K. Adachi, I. Yamada, K. N. Sato, K. Kawahata, A. Nishizawa, S. Ohdachi, K. Sato, T. Seki, T. Watari, J. Xu, A. Ejiri, S. Hirokura, K. Ida, Y. Kawasumi, M. Kojima, H. Sakakita, T. Ido, K. Kitachi, J. Koog and H. Kuramoto,
Observation of Dusts by Laser Scattering Method in theJIPPT-IIU Tokamak Mar. 1997

NIFS-486 S. Bazdenkov, T. Sato and The Complexity Simulation Group,
Topological Transformations in Isolated Straight Magnetic Flux Tube; Mar. 1997

NIFS-487 M. Okamoto,
Configuration Studies of LHD Plasmas; Mar. 1997

NIFS-488 A. Fujisawa, H. Iguchi, H. Sanuki, K. Itoh, S. Lee, Y. Hamada, S. Kubo, H. Idei, R. Akiyama, K. Tanaka, T. Minami, K. Ida, S. Nishimura, S. Morita, M. Kojima, S. Hidekuma, S.-I. Itoh, C. Takahashi, N. Inoue, H. Suzuki, S. Okamura and K. Matsuoka,
Dynamic Behavior of Potential in the Plasma Core of the CHS Heliotron/Torsatron; Apr. 1997

NIFS-489 T. Ohkawa,
Pfirsch - Schlüter Diffusion with Anisotropic and Nonuniform Superthermal Ion Pressure; Apr. 1997

NIFS-490 S. Ishiguro and The Complexity Simulation Group,
Formation of Wave-front Pattern Accompanied by Current-driven Electrostatic Ion-cyclotron Instabilities; Apr. 1997

NIFS-491 A. Ejiri, K. Shinohara and K. Kawahata,
An Algorithm to Remove Fringe Jumps and its Application to Microwave Reflectometry; Apr. 1997

NIFS-492 K. Ichiguchi, N. Nakajima, M. Okamoto,
Bootstrap Current in the Large Helical Device with Unbalanced Helical Coil Currents; Apr. 1997

NIFS-493 S. Ishiguro, T. Sato, H. Takamaru and The Complexity Simulation Group,
V-shaped dc Potential Structure Caused by Current-driven Electrostatic Ion-cyclotron Instability; May 1997

NIFS-494 K. Nishimura, R. Horiuchi, T. Sato,
Tilt Stabilization by Energetic Ions Crossing Magnetic Separatrix in Field-Reversed Configuration; June 1997

NIFS-495 T. -H. Watanabe and T. Sato,
Magnetohydrodynamic Approach to the Feedback Instability; July 1997

NIFS-496 K. Itoh, T. Ohkawa, S. -I.Itoh, M. Yagi and A. Fukuyama
Suppression of Plasma Turbulence by Asymmetric Superthermal Ions; July 1997

NIFS-497 T. Takahashi, Y. Tomita, H. Momota and Nikita V. Shabrov,
Collisionless Pitch Angle Scattering of Plasma Ions at the Edge Region of an FRC; July 1997

NIFS-498 M. Tanaka, A.Yu Grosberg, V.S. Pande and T. Tanaka,
Molecular Dynamics and Structure Organization in Strongly-Coupled Chain of Charged Particles; July 1997

NIFS-499 S. Goto and S. Kida,
Direct-interaction Approximation and Reynolds-number Reversed Expansion for a Dynamical System; July 1997

NIFS-500 K. Tsuzuki, N. Inoue, A. Sagara, N. Noda, O. Motojima, T. Mochizuki, T. Hino and T. Yamashina,
Dynamic Behavior of Hydrogen Atoms with a Boronized Wall; July 1997

NIFS-501 I. Viniar and S. Sudo,
Multibarrel Repetitive Injector with a Porous Pellet Formation Unit; July 1997

NIFS-502 V. Vdovin, T. Watari and A. Fukuyama,
An Option of ICRF Ion Heating Scenario in Large Helical Device; July 1997